ADVANCED MATERIALS
www.advmat.de

Surface Hydrophobization Provides Hygroscopic Supramolecular Plastics Based on Polysaccharides with Damage-Specific Healability and Room-Temperature Recyclability

Hongjun Jin, Weilin Lin, Ziyan Wu, Xinyu Cheng, Xinyuan Chen, Yingjie Fan, Wangchuan Xiao, Jianbin Huang, Qingrong Qian, Qinghua Chen, and Yun Yan**

Supramolecular materials with room-temperature healability and recyclability are highly desired because they can extend materials lifetimes and reduce resources consumption. Most approaches toward healing and recycling rely on the dynamically reversible supramolecular interactions, such as hydrogen, ionic and coordinate bonds, which are hygroscopic and vulnerable to water. The general water-induced plasticization facilitates the healing and reprocessing process but cause a troubling problem of random self-adhesion. To address this issue, here it is reported that by modifying the hygroscopic surfaces with hydrophobic alkyl chains of dodecyltrimethoxysilane (DTMS), supramolecular plastic films based on commercial raw materials of sodium alginate (SA) and cetyltrimethylammonium bromide (CTAB) display extraordinary damage-specific healability. Owing to the hydrophobic surfaces, random self-adhesion is eliminated even under humid environment. When damage occurs, the fresh surfaces with ionic groups and hydroxyl groups expose exclusively at the damaged site. Thus, damage-specific healing can be readily facilitated by water-induced plasticization. Moreover, the films display excellent room-temperature recyclability. After multiple times of reprocessing and re-modifying with DTMS, the rejuvenated films exhibit fatigueless mechanical properties. It is anticipated that this approach to damage-specific healing and room-temperature recycling based on surface hydrophobization can be applied to design various of supramolecular plastic polysaccharides materials for building sustainable societies.

1. Introduction

Supramolecular assembling materials with healability and recyclability have attracted great attention due to the growing concern over the global plastic pollution.[1–7] These supramolecular materials are considered to effectively extend service life and improve recycling rate through readily repairing and reprocessing, which will make significant contribution to realize a sustainable society.[8–11] Different from the traditional plastics based on extremely stable covalent bonds and cross-links, supramolecular plastic materials incorporate weak intermolecular interactions such as ionic interactions,[12–14] hydrogen bonds[5–8,15–18] and coordination interactions,[19–22] which have been well-established to achieve self-healing and reprocessing due to the reversible and dynamic nature of weak supramolecular forces.[23] It should be noted that these weak interactions are generally polar and vulnerable to water.[24–27] In many cases, the essence of efficient self-healing and reprocessing for supramolecular polymeric materials are ascribed to the readily water absorption and water-induced plasticization, which results in strongly self-adhering.[28–32] However, the water-assisted self-adhering process occurs non-specifically at the damage sites. Undesired self-adhesion generally occurs beyond the damaged sites when the ambient humidity gets high or the materials are exposed to water, which makes the storage and use demand harsh dry condition. Thus, to eliminate undesired self-adhesion,

H. Jin, W. Lin, Z. Wu, X. Cheng, X. Chen, Y. Fan, Q. Qian, Q. Chen
Engineering Research Center of Polymer Green Recycling of Ministry of Education
College of Environmental and Resource Sciences
College of Carbon Neutral Modern Industry
Fujian Normal University
Fuzhou, Fujian 350007, China
E-mail: cqhuar@fjnu.edu.cn

The ORCID identification number(s) for the author(s) of this article can be found under https://doi.org/10.1002/adma.202207688.

DOI: 10.1002/adma.202207688

H. Jin, J. Huang, Y. Yan
Beijing National Laboratory for Molecular Sciences (BNLMS)
College of Chemistry and Molecular Engineering
Peking University
Beijing 100871, China
E-mail: yunyan@pku.edu.cn

W. Lin, X. Cheng, X. Chen, Y. Fan, W. Xiao
School of Resources and Chemical Engineering
Sanming University
Sanming, Fujian 365004, China

supramolecular plastics with damage-specific healability are of great practical significance.

Within the past decades, multitudinous healable materials have emerged.[33–36] One of the approaches by releasing healing agents encapsulated in a polymer matrix by crack propagation allows for fracture site-specific repair.[37,38] However, in the majority of cases the healed zone is chemically distinct from the bulk materials. Besides, the healing process needs high temperature and can be repeated only limited times in principle. In contrast, the approach based on supramolecular assembly enable materials to heal many times even at room temperature, because of the intrinsic reversible and dynamic weak interactions.[23,33] The booming development of supramolecular assembling materials has promoted the design of supramolecular networks with intrinsic healability. However, these healable supramolecular materials are usually soft and tacky especially under high relative humidity (RH) due to the water-induced plasticization, which results in distinct mechanical strength decrease and randomly self-adhesion. Lately, some researchers dedicated to healable supramolecular materials with high strength in watery environment and remarkable achievements were made.[6,7,16,17,39] However, the general problem of undesired self-adhesion caused by the ubiquitous reversible and dynamic interactions has drawn little attention.

Recently, we developed a solid-phase molecular self-assembly (SPMSA) strategy to fabricate supramolecular film materials using commercially available polyelectrolytes (PE) and surfactants (SAa).[40–45] Compared to the conventional solution casting and hot compression molding methods for thin film fabrication, SPMSA provides a green and efficient way to fabricate large-scale supramolecular films. However, owing to the abundant ionic bonds, the obtained PE-SAa films display distinct hygroscopicity. The absorbed water bonds to the polar ionic groups and significantly weaken the electrostatic interactions between the oppositely charged groups of PE and SAa. This remarkably improves the reversible disengagement and recombination of the electrostatic bindings, which endows the supramolecular plastic films with water-enabled room-temperature mendability and recyclability,[40,41] but also undesired self-adhesion. Thus, in this work we propose a facile strategy to eliminate random self-adhesion and achieve damage-specific healing through grafting hydrophobic alkyl chains on the hygroscopic surfaces of the supramolecular plastic films fabricated via SPMSA with sodium alginate (SA) and cetyltrimethylammonium bromide (CTAB) (**Scheme 1**). The alkyl chains provided by dodecyltrimethoxysilane (DTMS) are supposed to turn the hygroscopic surface into hydrophobic and keep it non-tacky even under high RH. Meanwhile, the ionic and hydrogen bonds inside the film materials are still hygroscopic and the dynamic reversibility can be promoted by the absorbed water. In consequence, the self-adhesion occurs specifically at the damage sites where ionic groups and hydroxyl groups are re-exposed. These surface hydrophobized films also display room-temperature recyclability and the rejuvenated films show almost no mechanical decrease after multiple times recycling. Therefore, SA-CTAB plastic films with damage-specific healability and room-temperature recyclability was achieved through the facile strategy of surface hydrophobization. This strategy is universal for hygroscopic films based on polysaccharides. We expect the present work to be promising to boost the development and practical application of self-healable and recyclable supramolecular plastic materials.

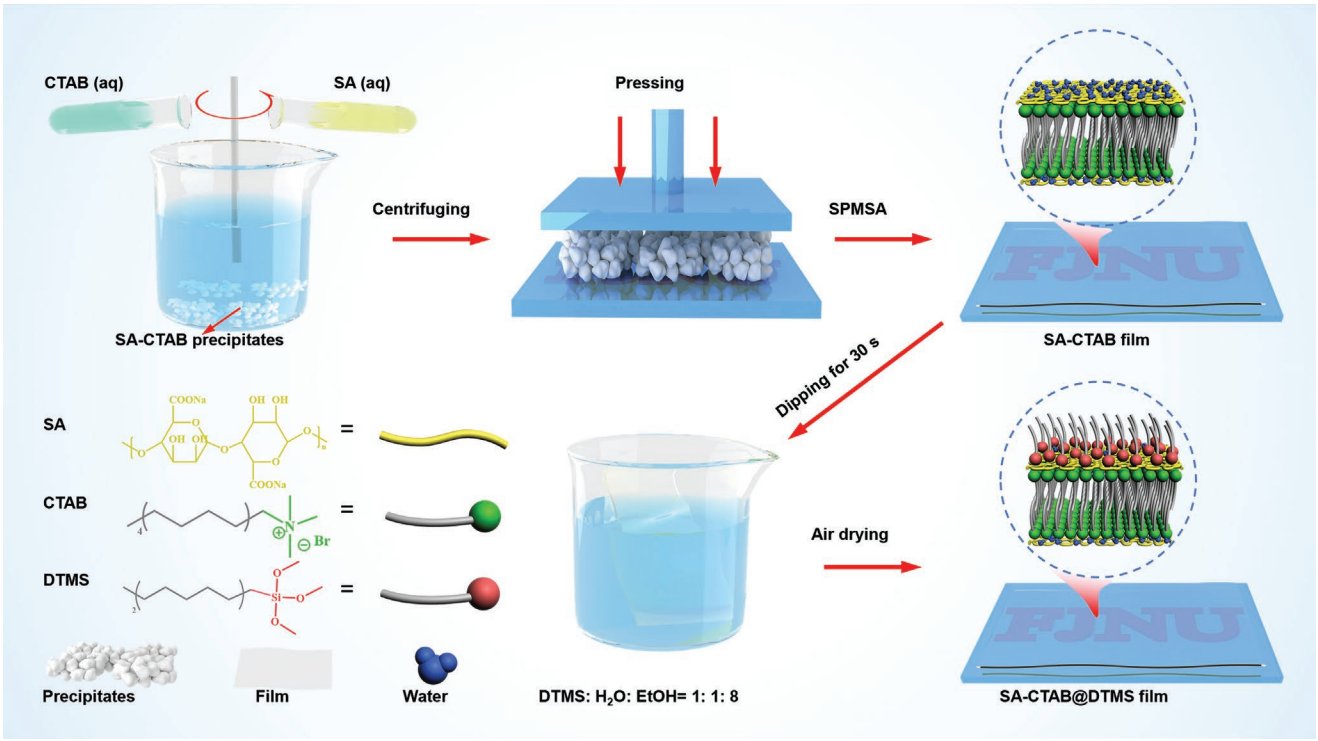

Scheme 1. Illustration of the solid phase molecular self-assembly (SPMSA) for preparing SA-CTAB film and the surface hydrophobization via grafting DTMS on the film surface.

2. Results and Discussion

The SA-CTAB supramolecular film was prepared via our previously reported SPMSA strategy. Generally, the aqueous solutions of SA and CTAB were first mixed at charge balancing ratio and white precipitates occurred immediately. Then, the precipitates were collected and separated through centrifuging. Under mechanical pressure around 0.5 MPa, the wet precipitates were forced to form a compact cake, which gradually transforms into a self-supporting and transparent film within 1 h at room temperature (Scheme 1).

Large-scale SA-CTAB films can be readily prepared using a domestic noodle machine (**Figure 1**a). Different from the precipitates that are dark under polarized optical microscopy

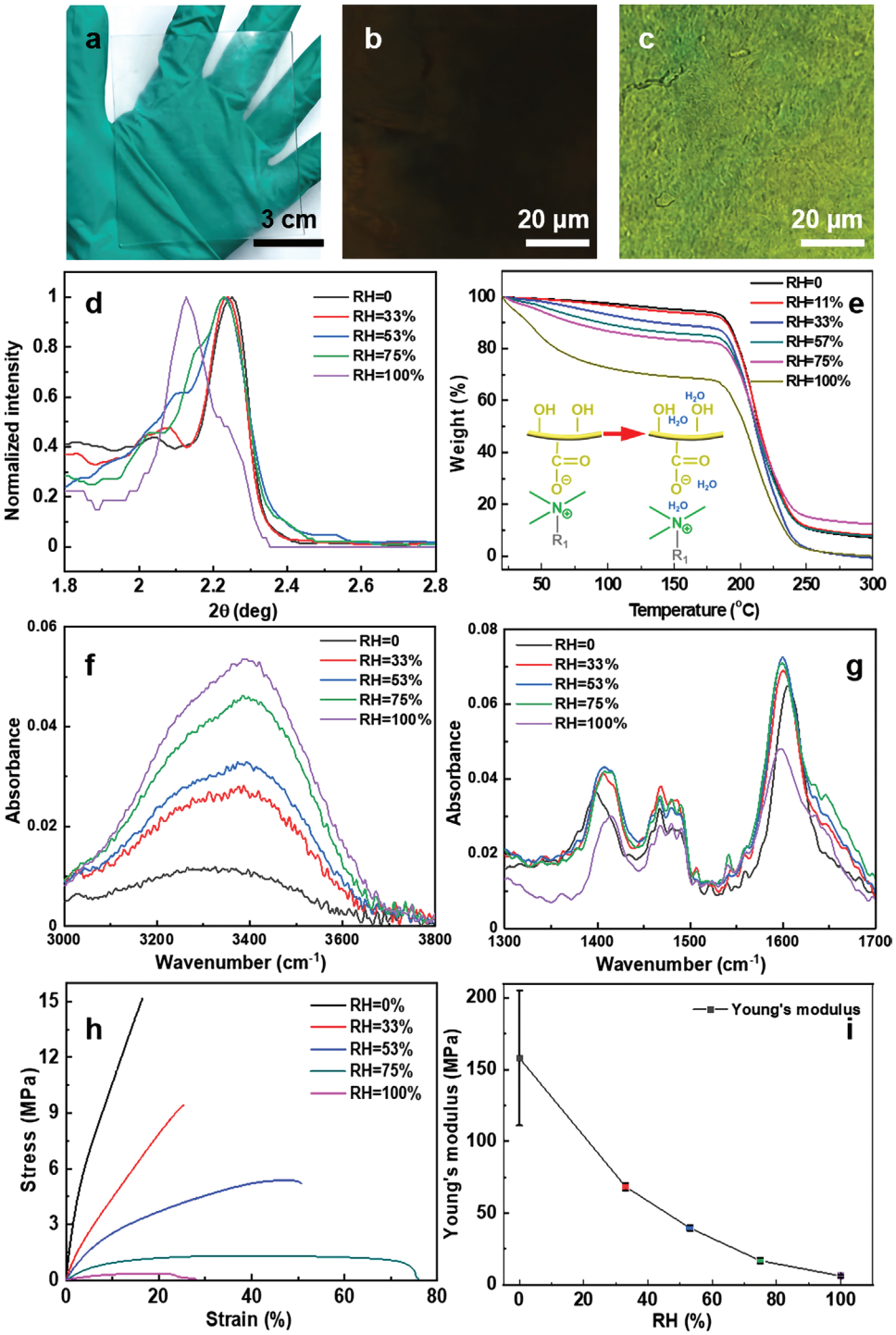

Figure 1. a) Photo of the 80 mm × 100 mm × 0.5 mm SA-CTAB film fabricated by using noodle machine. b,c) The birefringence of the SA-CTAB precipitates and film observed by POM, respectively. d) XRD pattern, e) TGA curves, f,g) FT-IR spectra, h) stress–strain curves and i) Young's modulus of the SA-CTAB films under RH of 0, 33%, 53%, 75%, and 100%, respectively.

(POM), the SA-CTAB film displays strong birefringence, indicating that molecules rearrange during the film formation (Figure 1b–c). X-ray diffraction (XRD) shows that the dry film has a distinct diffraction at $2\theta = 2.25°$ (Figure 1d). The corresponding d value (3.92 nm) is slightly shorter than twice the extending length of CTAB molecules (2.29 nm), indicating the formation of ordered lamellar phase with staggered alkyl chains. Thus, the SA chains are electrostatically bonded to the charged groups of CTAB and covered between the CTAB bilayers. Interestingly, when the films are stored in humid environment, the diffraction peak gradually shifts to lower angle and the d value increases in line with the increasing RH (Figure 1d; Table S1, Supporting Information). When the RH increases to 100%, the diffraction notably shift to $2\theta = 2.13°$ and the d value increase to 4.15 nm. The thermogravimetric analysis (TGA) and the Fourier transform infrared (FT-IR) spectra show that with the increasing RH, the water content in the SA-CTAB films increases correspondingly (Figure 1e,f; Table S1, Supporting Information). Under 100% RH, the water content reaches 32%, indicating the strong hygroscopicity of SA-CTAB film. The absorbed water molecules insert into the hydrophilic domains of the lamellar phase (Figure 1e inset), resulting in the increased interlayer spacing.

Furthermore, the absorbed water significantly weakens the electrostatic interactions between the oppositely charged groups of SA and CTAB as demonstrated by the FT-IR spectra in Figure 1g. The characteristic vibrations around 1400 and 1600 cm^{-1} are assigned to the symmetrical stretching vibration (ν_s) and asymmetric stretching vibration (ν_{as}) for COO^- of SA, respectively. COO^- groups that are highly bonded to quaternary ammonium (N^+) of CTAB have a lower vibrational frequency because of the less damping of the COO^- ν_s. The absorbed water weakens the bonding between COO^- and N^+, resulting in an upshift for the COO^- ν_s and an opposite change for the COO^- ν_{as} (Table S2, Supporting Information).[46] Moreover, with the increasing RH, the tensile breaking strength and Young's modulus decreases while the breaking elongation increases (Figure 1h,i; Table S3, Supporting Information). Under extremely high RH, the elongation suddenly decrease due to breaking occurs at the tensile fixtures. Thus, the absorbed water works as plasticizer to weaken the electrostatic interactions and enhance the molecular mobility.

Water-induced plasticization endows SA-CTAB films with appreciable self-healability. To demonstrate this property, we deliberately damaged the film with a thickness of 0.7 mm by cutting with a depth of 0.5 mm (**Figure 2**a). The damage sites were subsequently wetted with a drop of water and slightly pressed together. The damage markedly self-adhered and self-healed after 24 h as shown in Figure 2b–d. Figure 2e and Figure S1 (Supporting Information) show the stress–strain curves of the original, healed, and damaged films under different RH. The recovered breaking strength, elongation and

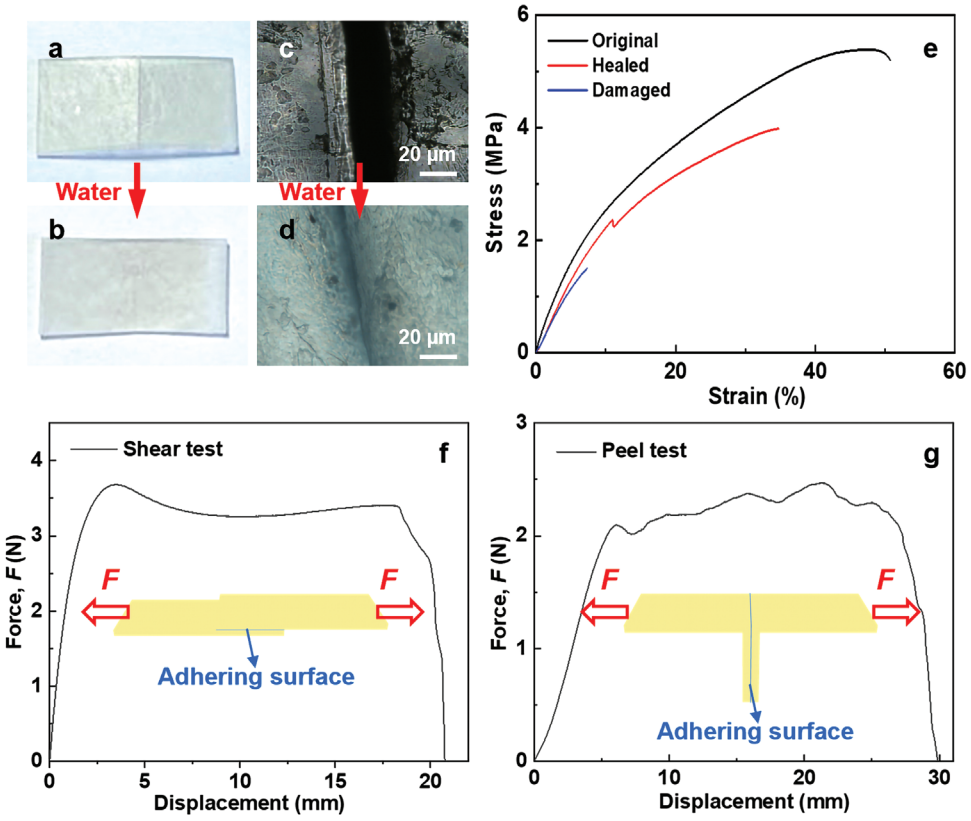

Figure 2. a,b) Photos of the damaged SA-CTAB film (a) and the healed film after wetting with a drop of water and slightly pressing together, and then storing under RH 53% for 24 h (b). c,d) POM bright field images of the damaged film (c) and the healed film (d). e) Stress–strain curves of the original, healed, and damaged SA-CTAB films, respectively. f,g) Force–displacement curves of the shear test (f) and the peel test (g) for the self-adhered films, respectively.

toughness under RH 53%, which is close to mean annual RH in the dry northern China, are 76% ± 5%, 72% ± 4%, and 47% ± 4%, respectively. The healing efficiency can be determined by the recovered toughness of the healed film, which increases with the increasing RH (Figure S2 and Table S4, Supporting Information). However. this water-assisted self-adhering also occurs at undamaged sites which causes serious problem in film storage and use. To evaluate the self-adhesion ability, shear test and peel test were conducted to measure the shear strength and interfacial toughness according to literature.[47] Under 100% RH, the intact films were readily adhered by pressing the 1 cm × 1 cm area with 1 kg weight for 5 min. The shear strength and interfacial toughness could be determined by the mean force at plateau of the force–displacement curves (Figure 2f,g), which are 34 kPa and 454 J m^{-2}, respectively. Either by shearing or peeling the adhered films cause irreversible deformation, which greatly impedes the practical application.

In order to avoid the ubiquitous self-adhesion and keep the film non-tacky under high RH, surface hydrophobization with alkyl chains were designed to protect the intact surface from water-induced plasticization. Owing to the abundant hydroxyl groups on SA molecules, siloxane DTMS is supposed to be grafted on the film through hydrolysis reactions. As shown in Scheme 1, DTMS modified SA-CTAB (SA-CTAB@DTMS) film can be readily obtained by dipping the SA-CTAB film into DTMS solution (DTMS:H_2O:EtOH = 1:1:8, volume ratio) for 30 s and then air drying at room temperature. The composition of the treating solution was chosen according to the solubility and hydrolysis rate of DTMS (Figure S3, Supporting Information). The contact angle tests, scanning electron microscopy (SEM) images and X-ray photoelectron spectroscopy (XPS) demonstrate the successful modification of DTMS. **Figure 3**a and Table S3 (Supporting Information) show the contact angles between SA-CTAB film and water decrease from 96° to 53° as the RH increases from 0 to 100%, indicating that the film surface is gradually hydrated under higher RH. As a comparison, the contact angles of the SA-CTAB@DTMS films are all about 110° under different RH. SEM images show that the surface of SA-CTAB film is pretty smooth (Figure 3c), while the surface of SA-CTAB@DTMS forms irregular layered structures and turns to be very rough (Figure 3d). XPS spectra also manifest the successful modification of DTMS as silicon is significantly enhanced after coating (Figure 3e; Figure S4, Supporting Information). The alkyl chains of DTMS turn the hygroscopic surface into hydrophobic and non-tacky, which effectively prevents the water-assisted self-adhesion of intact surfaces. Comparing to SA-CTAB films which are easily adhering to each other under high RH (Figure 3f; Figure S5a, Supporting Information), SA-CTAB@DTMS films remain individual even by applying a pressure about 0.1 MPa under 100% RH (Figure 3g; Figure S5b, Supporting Information). This strategy is universal for hygroscopic films comprised with polysaccharides such as sodium carboxymethylcellulose (CMC) and chitosan quaternary ammonium salt (QCS), but unsuitable for polyelectrolytes without hydroxyl groups (Figure S6, Supporting Information). Notably, the SA-CTAB@DTMS films retain self-healing ability. When the film is damaged, fresh surfaces expose. The fresh surfaces are free of DTMS but possess abundant ionic groups and hydroxyl

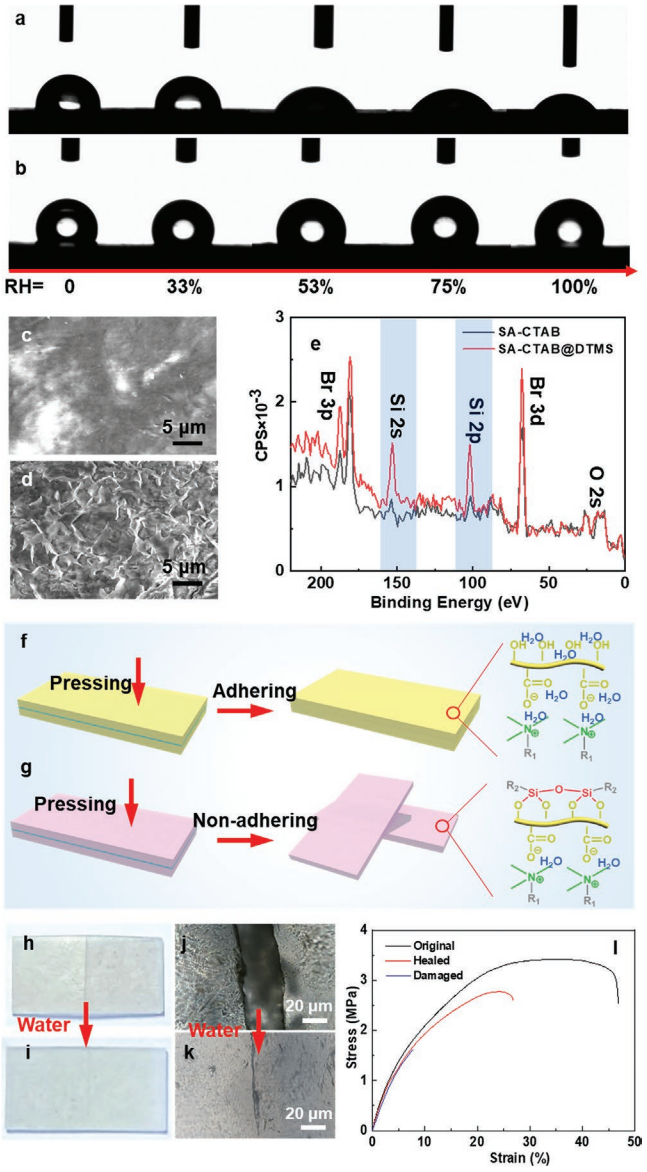

Figure 3. a,b) Contact angle tests of SA-CTAB films (a) and SA-CTAB@DTMS films (b) under RH of 0, 33%, 53%, 75%, and 100%, respectively. c,d) SEM images of the surfaces of SA-CTAB film (c) and SA-CTAB@DTMS film (d). e) XPS spectra of SA-CTAB film and SA-CTAB@DTMS film. f,g) Illustration of the self-adhering process of SA-CTAB films (f) and SA-CTAB@DTMS films (g). The SA-CTAB films are strongly adhered to each other while the SA-CTAB@DTMS films remain individual. h) Photo of the damaged SA-CTAB@DTMS film by deliberately cutting with a depth of 0.5 mm. i) Photo of the healed film after wetting with a drop of water and slightly pressed together, and then storing under RH 53% for 24 h. j,k) POM bright field images of damaged film (j) and the healed film (k). l) Stress–strain curves of the original, healed and damaged SA-CTAB@DTMS films, respectively.

groups. Under high RH, SA-CTAB@DTMS films absorb water from environment, which further enhance the dynamics of the intermolecular weak interactions. Thus, the damaged films can be effectively repaired as shown in Figure 3h–k. Figure 3l and Figure S7 (Supporting Information) are the stress–strain curves of the original, healed, and damaged SA-CTAB@DTMS

films under different RH. The recovered breaking strength, elongation and toughness under RH 53% are 88% ± 10%, 50% ± 4%, and 38% ± 7%, respectively. The healing efficiencies also increase with the increasing RH (Figure S8 and Table S6, Supporting Information), which are just slightly lower than that of SA-CTAB films. Thus, damage-specific healing is achieved by simply modifying the film surfaces with hydrophobic alkyl chains.

The damage-specific healability derives from the hygroscopicity of SA-CTAB@DTMS films, despite the surfaces are

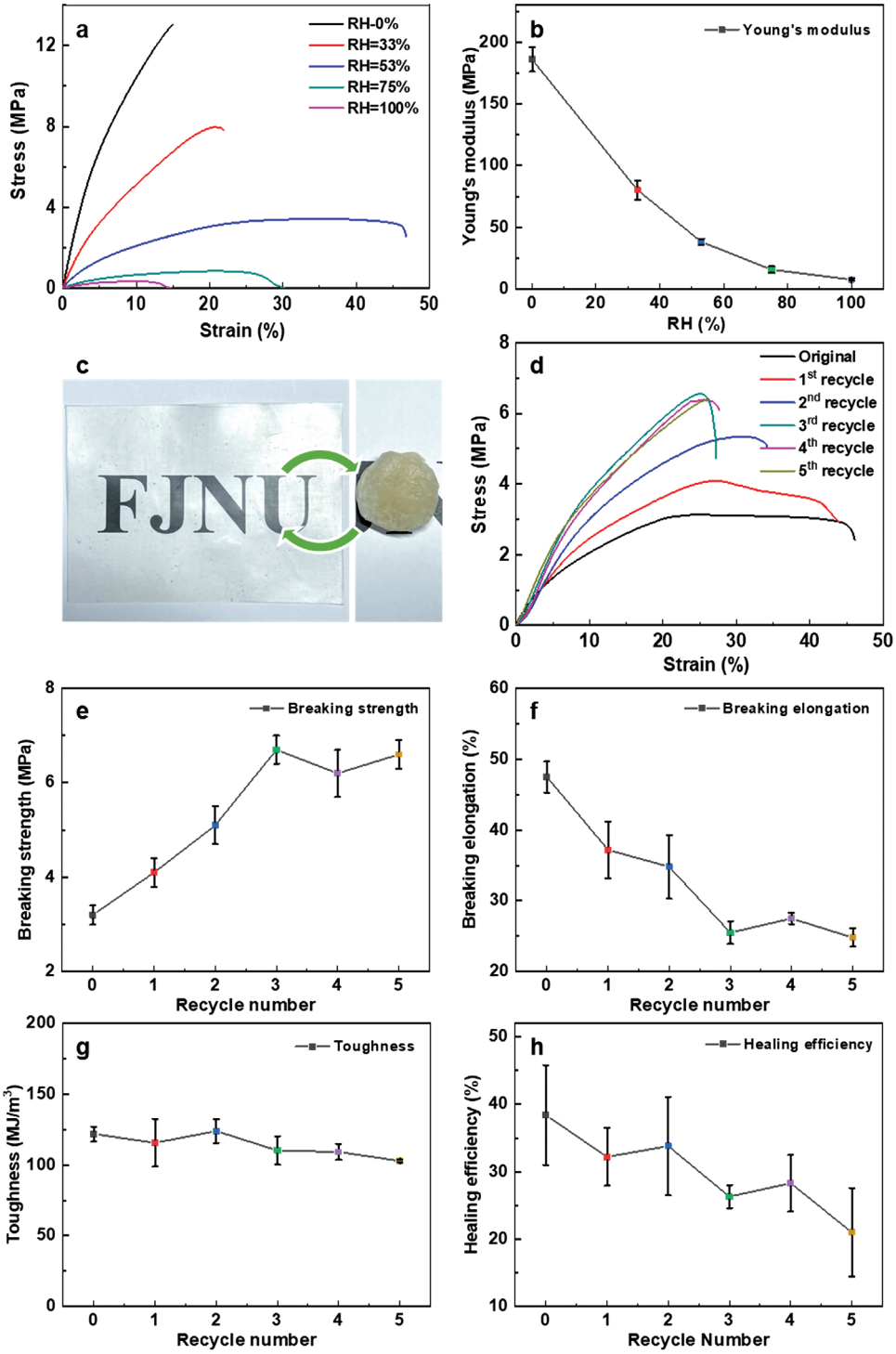

Figure 4. a) Stress–strain curves and b) Young' modulus of the SA-CTAB@DTMS films under RH of 0, 33%, 53%, 75%, and 100%, respectively. c) The recycle process of the SA-CTAB@DTMS films. d) Stress–strain curves, e) breaking strength, f) breaking elongation, g) toughness, and h) healing efficiency of the SA-CTAB@DTMS films after multiple recycling and re-modifying with DTMS.

hydrophobic. Under RH of 100%, the SA-CTAB@DTMS film absorb 27% of water, which is just slightly lower than that of the pristine SA-CTAB film (Figure S9, Supporting Information). The thickness of the DTMS-modified area is about 50 μm as the SEM cross section images show (Figure S10, Supporting Information). The water uptake capacity for the SA-CTAB@DTMS film with thickness of 0.7 mm is supposed to decrease $(0.5 \times 2)/0.7 = 14\%$, which coincides with the TGA results. Contact angle tests further confirm that inside the SA-CTAB@DTMS film is still hydrophilic (Figure S11, Supporting Information). Thus, beyond the DTMS-modified area, the inner body of the film maintains strong hygroscopicity. Meanwhile, the absorbed water can also work as plasticizer to enhance the dynamics of ionic bonds and the molecular mobility, which was further verified by the stress–strain tests. As **Figure 4**a,b and Table S7 (Supporting Information) show, the breaking strength and Young's modulus decreases with the increasing RH, while the breaking strain remarkably increases. It is worth noting that the dry SA-CTAB@DTMS film maintains lamellar structure but with an increased interlayer spacing to 4.02 nm, which is unchanged under higher RH (Figure S12, Supporting Information). Thus, the decrease in mechanical properties after modifying DTMS may be attributed to the larger spacing. Under higher RH, the absorbed water molecules insert into the spacing and further weaken the ionic interactions and mechanical strength. Furthermore, this water-induced plasticization also endows the film with excellent room-temperature recyclability. With the aid of drops of water, the film can be crumpled up into a ball and then rejuvenate into new film by repeatedly pressing and modifying at room temperature (Figure 4c). Amazingly, despite the breaking strength of the recycled films increases and the elongation decreases in the first two cycles, the toughness of the recycled films shows little change (Figure 4d–g). And after three times of recycle and modification, the mechanical properties of the recycled films become stable and are not fatigued, which confirmed the excellent room-temperature recyclability. Owing to the increasing content of DTMS which results in depletion of hydroxyl groups and decrease of hygroscopicity, the healing efficiency of the recycled film gradually decreases with recycle number. After 5 times recycling, the healing efficiency decreases about 45% (Figure 4h).

3. Conclusion

We have demonstrated a facile strategy of surface hydrophobization to generate damage-specific healable and room-temperature recyclable supramolecular plastic films, prepared through our recently reported solid-phase molecular self-assembly (SPMSA) strategy based on sodium alginate (SA) and cetyltrimethylammonium bromide (CTAB). In order to eliminate undesired self-adhesion under high relative humidity, dodecyltrimethoxysilane (DTMS) was designed to graft on the SA-CTAB films through hydrolysis reacting with the surface hydroxyl groups provided by SA molecules, which turns the hygroscopic surface into hydrophobic. Thus, self-adhesion occurs exclusively at the damage sites when fresh surfaces expose, exhibiting damage-specific healability. Furthermore, the SA-CTAB@DTMS films can be reprocessed with the aid of drops of water at room temperature. After multiple times of reprocessing and re-modifying with DTMS, the recycled SA-CTAB@DTMS films show little fatigue in mechanical properties, manifesting the excellent room-temperature recyclability. This strategy is universal for various hygroscopic supramolecular plastics with functional groups able to reaction with DTMS. For supramolecular plastics with other functional groups, we expect other hydrophobic agents should be utilized. Thus, we have established a novel method leading to damage-specific healable and room-temperature recyclable supramolecular plastic films, which opens up opportunities for practical applications of supramolecular plastic materials.

Supporting Information

Supporting Information is available from the Wiley Online Library or from the author.

Acknowledgements

This work was supported financially by the National Natural Science Foundation of China (NSFC 22172004, NSFC 21972003) and the Department of Education, Fujian Province (JAT210049).

Conflict of Interest

The authors declare no conflict of interest.

Data Availability Statement

The data that support the findings of this study are available from the corresponding author upon reasonable request.

Keywords

damage-specific healing, plasticization, supramolecular films, surface hydrophobization, water

Received: August 23, 2022
Revised: November 6, 2022
Published online:

[1] P. Cordier, F. Tournilhac, C. Soulie-Ziakovic, L. Leibler, *Nature* **2008**, *451*, 977.
[2] M. Burnworth, L. Tang, J. R. Kumpfer, A. J. Duncan, F. L. Beyer, G. L. Fiore, S. J. Rowan, C. Weder, *Nature* **2011**, *472*, 334.
[3] H. Liu, W. Wei, L. Zhang, J. Xiao, J. Pan, Q. Wu, S. Ma, H. Dong, L. Yu, W. Yang, D. Wei, H. Ouyang, Y. Liu, *Adv. Funct. Mater.* **2021**, *31*, 2104088.
[4] Q. Zhang, Y. X. Deng, H. X. Luo, C. Y. Shi, G. M. Geise, B. L. Feringa, H. Tian, D. H. Qu, *J. Am. Chem. Soc.* **2019**, *141*, 12804.
[5] Y. Yanagisawa, Y. Nan, K. Okuro, T. Aida, *Science* **2018**, *359*, 72.
[6] Y. Li, S. Li, J. Sun, *Adv. Mater.* **2021**, *33*, 2007371.
[7] Y. Fujisawa, A. Asano, Y. Itoh, T. Aida, *J. Am. Chem. Soc.* **2021**, *143*, 15279.

[8] W. Niu, Y. Zhu, R. Wang, Z. Lu, X. Liu, J. Sun, *ACS Appl. Mater. Interfaces* **2020**, *12*, 30805.
[9] J. Han, Y. F. Guo, H. Wang, K. Zhang, D. Yang, *J. Am. Chem. Soc.* **2021**, *143*, 19486.
[10] B. Qin, P. Sun, B. Tang, Z. Yin, X. Cao, Q. Chen, J. F. Xu, X. Zhang, *Adv. Mater.* **2020**, *32*, 2000096.
[11] Q. Xia, C. Chen, Y. Yao, J. Li, S. He, Y. Zhou, T. Li, X. Pan, Y. Yao, L. Hu, *Nat. Sustainability* **2021**, *4*, 627.
[12] Y. Miwa, K. Taura, J. Kurachi, T. Udagawa, S. Kutsumizu, *Nat. Commun.* **2019**, *10*, 1828.
[13] Y. Deng, Q. Zhang, B. L. Feringa, H. Tian, D.-H. Qu, *Angew. Chem., Int. Ed.* **2020**, *132*, 5316.
[14] M. M. Obadia, B. P. Mudraboyina, A. Serghei, D. Montarnal, E. Drockenmuller, *J. Am. Chem. Soc.* **2015**, *137*, 6078.
[15] H. Wang, H. Liu, Z. Cao, W. Li, X. Huang, Y. Zhu, F. Ling, H. Xu, Q. Wu, Y. Peng, B. Yang, R. Zhang, O. Kessler, G. Huang, J. Wu, *Proc. Natl. Acad. Sci. USA* **2020**, *117*, 11299.
[16] J. Kang, D. Son, G. N. Wang, Y. Liu, J. Lopez, Y. Kim, J. Y. Oh, T. Katsumata, J. Mun, Y. Lee, L. Jin, J. B. Tok, Z. Bao, *Adv. Mater.* **2018**, *30*, 1706846.
[17] H. Wei, Y. Yang, X. Huang, Y. Zhu, H. Wang, G. Huang, J. Wu, *J. Mater. Chem. A* **2020**, *8*, 9013.
[18] J. Zhu, G. Y. Chen, L. Yu, H. Xu, X. Liu, J. Sun, *CCS Chem.* **2020**, *2*, 280.
[19] C. H. Li, C. Wang, C. Keplinger, J. L. Zuo, L. Jin, Y. Sun, P. Zheng, Y. Cao, F. Lissel, C. Linder, X. Z. You, Z. Bao, *Nat. Chem.* **2016**, *8*, 618.
[20] J. Fan, J. Huang, Z. Gong, L. Cao, Y. Chen, T. Robust, *ACS Appl. Mater. Interfaces* **2021**, *13*, 1135.
[21] M. Xie, Y. Che, K. Liu, L. Jiang, L. Xu, R. Xue, M. Drechsler, J. Huang, B. Z. Tang, Y. Yan, *Adv. Funct. Mater.* **2018**, *28*, 1803370.
[22] C. H. Li, J. L. Zuo, *Adv. Mater.* **2020**, *32*, 1903762.
[23] R. Hoogenboom, *Angew Chem Int Ed Engl* **2012**, *51*, 11942.
[24] C. F. J. Faul, M. Antonietti, *Adv. Mater.* **2003**, *15*, 673.
[25] R. Zhang, Y. Zhang, H. S. Antila, J. L. Lutkenhaus, M. Sammalkorpi, *J. Phys. Chem. B* **2017**, *121*, 322.
[26] X. Lyu, A. M. Peterson, *Macromolecules* **2018**, *51*, 10003.
[27] P. Batys, Y. Zhang, J. L. Lutkenhaus, M. Sammalkorpi, *Macromolecules* **2018**, *51*, 8268.
[28] A. B. South, L. A. Lyon, *Angew. Chem., Int. Ed.* **2010**, *49*, 767.
[29] X. Wang, F. Liu, X. Zheng, J. Sun, *Angew. Chem., Int. Ed.* **2011**, *50*, 11378.
[30] Y. Li, S. Chen, M. Wu, J. Sun, *Adv. Mater.* **2012**, *24*, 4578.
[31] Y. Du, W. -Z. Qiu, Z. L. Wu, P. -F. Ren, Q. Zheng, Z.-K. Xu, *Adv. Mater. Interfaces* **2016**, *3*, 1600167.
[32] Z. Shi, J. Kang, L. Zhang, *ACS Appl. Mater. Interfaces* **2020**, *12*, 23484.
[33] F. Herbst, D. Dohler, P. Michael, W. H. Binder, *Macromol. Rapid. Commun.* **2013**, *34*, 203.
[34] Y. Yang, X. Ding, M. W. Urban, *Prog. Polym. Sci.* **2015**, *49–50*, 34.
[35] N. Roy, B. Bruchmann, J. M. Lehn, *Chem. Soc. Rev.* **2015**, *44*, 3786.
[36] S. Wang, M. W. Urban, *Nat. Rev. Mater.* **2020**, *5*, 562.
[37] K. S. Toohey, N. R. Sottos, J. A. Lewis, J. S. Moore, S. R. White, *Nat. Mater.* **2007**, *6*, 581.
[38] S. R. White, N. R. Sottos, P. H. Geubelle, J. S. Moore, M. R. Kessler, S. R. Sriram, E. N. Brown, S. Viswanathan, *Nature* **2001**, *409*, 794.
[39] S. R. Ha, S. Park, J. T. Oh, D. H. Kim, S. Cho, S. Y. Bae, D. W. Kang, J. M. Kim, H. Choi, *Nanoscale* **2018**, *10*, 13187.
[40] H. Jin, M. Xie, W. Wang, L. Jiang, W. Chang, Y. Sun, L. Xue, S. Zang, J. Huang, Y. Yun, J. Lei, *CCS Chem.* **2020**, *2*, 98.
[41] H. Jin, C. Ma, W. Wang, Y. Cai, J. Qi, T. Wu, P. Liao, H. Li, Q. Zeng, M. Xie, J. Huang, Y. Yan, *ACS Mater. Lett.* **2021**, *4*, 145.
[42] W. Wang, M. Xie, H. Jin, W. Zhi, K. Liu, C. Ma, P. Liao, J. Huang, Y. Yun, *Mater. Chem. Front.* **2020**, *4*, 1530.
[43] P. Liao, T. Wu, H. Jin, W. Wang, J. Huang, B. Z. Tang, Y. Yan, *Nat. Commun.* **2021**, *12*, 5496.
[44] J. Qi, T. Wu, W. Wang, H. Jin, S. Gao, S. Jiang, J. Huang, Y. Yan, *Aggregate* **2022**, *3*, e173.
[45] X. Dou, H. Jin, T. Wu, J. Huang, B. Zhang, T. Chen, Z. Liu, Y. Yan, *J. Phys. Chem. B* **2022**, *126*, 6345.
[46] D. K. Beaman, E. J. Robertson, G. L. Richmond, *J. Phys. Chem. C* **2011**, *115*, 12508.
[47] H. Yuk, C. E. Varela, C. S. Nabzdyk, X. Mao, R. F. Padera, E. T. Roche, X. Zhao, *Nature* **2019**, *575*, 169.